Boletim da Sociedade Astronômica Brasileira, **33**, no. 1, 166-167

Dust modeling in red supergiants using Bayesian inference

T. de Amorim[1], A. Carciofi[1]

[1] Institute of Astronomy, Geophysics and Atmospheric sciences/University of São Paulo. e-mail: tajan.amorim@usp.br

Abstract. We present a detailed model of the characteristics of the dust grains around the red supergiant VY CMa. This star has a long observational history, and therefore a quite complete SED is available for this study. A novel approach here proposed is to combine the HDUST code, which performs the radiative transfer in dusty media, with a Bayesian inference based on Markov Chain Monte Carlo techniques (MCMC). The Bayesian inference allows for the many parameters involved in the modelling to be put in a seamless perspective, where the relative role of each one on shaping the SED, as well their cross-correlations, are apparent from the posterior probabilities provided by the MCMC method. Our results indicate that the dust surrounding VY CMa is quite dense, with $\tau_V \approx 5$. The circumstellar dust reprocesses $91.9 \pm 0.1\%$ of the stellar flux. The inner radius of the dust layer, $R_{\rm int} \approx 13.0\,R_\star$, corresponds to an equilibrium temperature of 1095 ± 25 K. The most probable parameters indicate the presence of grains with wide range of sizes ($0.47 \pm 0.17 < a < 363^{+26}_{-75}\,\mu$m) and a distribution associated with a power-law of $q = 3.63^{+0.03}_{-0.04}$. The value of q is especially interesting because it is very close to that found for the interstellar medium, suggesting that the grains around VY CMa share important commonalities to those of the interstellar medium.

Resumo. Apresentamos um modelo detalhado das características dos grãos de poeira na supergigante vermelha VY CMa. Esta estrela tem uma longa história de observação e, portanto, uma SED bastante completa está disponível para este estudo. Uma nova abordagem aqui proposta é combinar o código HDUST, que realiza a transferência radiativa, com a inferência Bayesiana baseada em técnicas de Markov Chain Monte Carlo (MCMC). A inferência bayesiana permite que os diversos parâmetros envolvidos na modelagem sejam colocados em perspectiva, obtendo o papel relativo de cada um na formação do SED, bem como suas correlações, aparentes a partir das probabilidades posteriores fornecidas pelo método MCMC. Nossos resultados indicam que a poeira em torno de VY CMa é bastante densa, com $\tau_V \approx 5$. A poeira circunstelar reprocessa $91.1 \pm 0.5\%$ do fluxo estelar. O raio interno da camada de poeira, $R_{\rm int} \approx 13.0\,R_\star$, corresponde a uma temperatura de equilíbrio de 1095 ± 25 K. Os parâmetros mais prováveis indicam a presença de grãos com ampla gama de tamanhos ($0.47 \pm 0.17 < a < 363^{+26}_{-75}\,\mu$m) e uma distribuição associada a uma lei de potência de $q = 3.63^{+0.03}_{-0.04}$. O valor de q é especialmente interessante porque é muito próximo ao encontrado para o meio interestelar, sugerindo que os grãos ao redor de VY CMa compartilham semelhanças importantes com aqueles do meio interestelar.

Keywords. Supergiants – dust, extinction – Methods: statistical

1. Introduction

It is estimated that massive stars ($M \gtrsim 8\ M_\odot$) lose more than half of their mass after they leave the main sequence, and a significant fraction of it occurs during the Red Supergiant (RSG) phase (**?**). This mass loss forms a very dense circumstellar outflow, where molecules and dust grains are produced once the gas cools down to sufficiently low temperatures. The site of molecular and dust formation is still not well known, as it depends on the gas temperature and the properties of the refractory material produced (**?**).

The dust grains affect the Spectral Energy Distribution (SED) of a star basically in two ways: they absorb radiation at shorter wavelengths (ultraviolet – UV – and visible) and reemit the energy in the infrared (IR) part of the spectrum. This process is known as "reprocessing", and causes the well-known IR excess observed in RSGs and other dusty objects such as young stellar objects (YSO), asymptotic giant branch (AGB) stars, etc. Thus, the SED, once corrected by the interstellar reddening, becomes a rich source of information about the central star and its circumstellar material and may, in some cases, be the only source about the dust itself.

The dust grain size is one of the main parameters that controls the reprocessing pattern of a grain population. However, it may be extremely difficult to determine its distribution using only the SED as explained by the concept of approximate invariance, this derives from the fact that differently sized grains have similar optical properties at long wavelengths, leading to similar SEDs, as shown by **?**. These authors studied the effects of grain size in the SED, showing that, under some conditions, the SEDs from models with different grain sizes may be very similar. The most important condition for this effect to hold is that different models have the same reprocessing optical depth and temperature. The reprocessing optical depth, $\tau_{\rm rep}$, is defined as

$$1 - e^{-\tau_{\rm rep}} \equiv \frac{L_{\rm rep}}{L_\star}\,, \tag{1}$$

where $L_\star$ is the stellar luminosity and $L_{\rm rep}$ is the fraction of the stellar luminosity that was reprocessed by the envelope. It follows from their work that, for a fixed grain temperature structure, the reprocessing optical depth is the only unambiguous parameter that can be extracted from the observations. Models that have very different grain sizes, and thus different optical properties, have a very similar SED because all models reprocess the same fraction of the stellar luminosity (approximately 10%, in this case). Another condition for approximate invariance to hold is that the optical properties of the grains have a similar shape in the spectral domain of interest. In practice, as discussed by **?**, this condition holds as long as the grain sizes considered are not widely different from each other.

In this contribution, our goal is to understand to what extent the SED can be used to infer the properties of the circumstellar grains (temperature, opacity, size distribution, etc.), taking into account the effect of the approximate invariance and applying the robust technique of Bayesian inference (Explained in Section 4). To achieve that, we selected the star VY Canis Majoris (VY

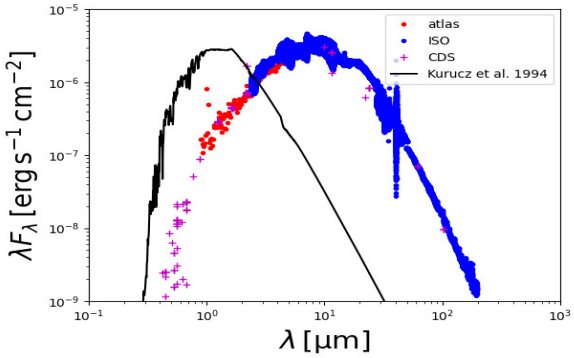

Figure 1. In black, a photospheric model with $T_{\rm eff}$ = 3500 K and log(g[cgs]) = 0 from **?**. The points correspond to VY CMa's observed SED. The data was taken from the Cassini Atlas Of Stellar Spectra (CAOSS, **?**), the Infrared Space Observatory (ISO) and the CDS portal [1].

CMa) as our main target due to the large amount of research built upon this star, resulting in a large amount of data available.

VY CMa, which is classified as a red supergiant star and thought to be near the end of its life, is one of the biggest stars in the known universe with a radius of 1420 $R_\odot$ (**?**). Because of its gigantic radius, it has a low superficial temperature, around $T_{\rm eff} \approx 3490$ K, which is compensated by its size granting it a luminosity of 270,000 $L_\odot$, one of the most luminous stars in the sky (**?**). Current observations suggest that VY CMa loses more than $2 \times 10^{-4}\,M_\odot yr^{-1}$ (**?**), which places it as the third brightest object in the sky at 10 μm (**?**), aside from the objects in our solar system. The presence of large grains in VY CMa's surroundings was observed by **?**. They suggest a maximum grain size of at least $a_{\rm max} = 0.5\,\mu$m. The material that was expelled by the star is typically organized in clumps around it, which can be observed by polarimetry. In this project however, we approximate the surrounding dust as a spherical shell, because the presence of clumps introduces a much more complex modelling effort.

2. Data

Fig. 1 represents the observed SED of VY CMa compared to a photospheric model (solid line) with $T_{\rm eff} = 3500$ K and log(g[cgs]) = 0 from **?**. The reprocessing effect can be seen, in this figure, as the SED in the IR domain lies much above the photospheric flux level, owing to dust emission. It is clear from the image that the dust visibly decreases the amount of UV light, by absorbing higher energy photons, and increasing the flux at longer wavelengths due to the grain thermal emission.

3. Model description

The central star parameters, as determined by **?**, were held fixed (Tab. 1). The stellar spectra of **?** was used to represent the stellar photospheric spectrum. To represent the reprocessing of the interstellar medium, we adopted the E(B-V) as a free parameter, ranging from 0 to 3.

To explore the dust grains properties around VY CMa, we computed the theoretical SEDs, for a large grid of models, using the HDUST code (**?**, **?**, **?**). HDUST is a Monte Carlo radiative transfer code that solves the coupled problem of the radiative transfer and radiative equilibrium in both gaseous and dusty media. The grid of models was build considering 5 parameters (their values are present in Table 2. In Section 5.1, we show the effect that each parameter has on the SED):

Table 1. Fixed parameters of this study. The stellar parameters are from **?**. $M_\star$ corresponds to stellar mass, $R_\star$ to stellar radius, $T_{\rm eff}$ to effective temperature, log(g) to the logarithm of the surface gravity, $V_{\rm rot}$ to rotational speed and d to distance from Earth.

$M_\star$[$M_\odot$]	$R_\star$[$R_\odot$]	$T_{\rm eff}$[K]	log(g)	$V_{\rm rot}$[km/s]	d[pc]
17	1420	3490	-0.6	40	1170

- Distribution of grain sizes: We have parameterized the grain size (a), which was assumed spherical, as a probability density function of the type,

$$f(a) = C(q)\, a^{-q}, a_{min} < a < a_{max}\,, \quad (2)$$

  where C is a normalization constant, q is the power-law exponent (the larger the q, the smaller the grains) and $a_{\rm min}$ and $a_{\rm max}$ are, respectively, the lower and upper bounds of the grain size distribution. $a_{\rm min}$, $a_{\rm max}$ and q were considered as free parameters within the range shown in the Tab. 2. Such function was first proposed in the pioneering work of **?** that used it to model the interstellar extinction law. They found q to be quite uniform around the value of 3.5 for many different lines of sight, indicating a common process for the formation of dust grains in the interstellar medium. Until now, more than 3000 articles have applied this distribution on their works, some of the most remarkable ones are **?**, **?** and **?**.
- Dust envelope: The dust envelope is considered in our models as a spherical shell, with an outer radius of $R_{\rm ext} = 200\,R_\star$ and internal radius, $R_{\rm int}$. As the temperature of the dust is one of the main parameters for the approximate invariance effect to hold (see Section 1), we have selected the value of $R_{\rm int}$ in order to obtain the corresponding grid values of the inner temperature, $T_{\rm int}$, which is the dust temperature at $r = R_{\rm int}$, where r is the distance from the center of the star. The grain number density within the shell (n) was parameterized by,

$$n = n_0 \cdot \left(\frac{R_{\rm int}}{r}\right)^2\,, \quad (3)$$

  where n_0 is the base number density.
- Optical depth: As explained in Section 1, due to the approximate invariance effect the main parameter that can be unambiguously obtained from the SED is the $\tau_{\rm rep}$. Therefore, we have considered it as a free parameter. The $\tau_{\rm rep}$ can be easily estimated from a HDUST simulation as follows. HDUST keeps track of the origin of the photons that escape the envelope. This origin can be either stellar emission or envelope emission. By integrating the total envelope emitted flux from the model, we obtain $L_{\rm rep}$ of Eq. 1.
- Grain composition: Although we have tested other optical constants, as the ones present in the DOCCD [2], we have found that the optical constants measured by **?**, for astronomical silicate grains, were consistent with the data and so were held fixed.

[1] ISO archive can be acessed in `http://nida.esac.esa.int/nida-cl-web/`. CDS portal, in `https://cdsportal.u-strasbg.fr/?target=VY%20CMa`.

[2] The Database of Optical Constants for Cosmic Dust can be acessed in `https://www.astro.uni-jena.de/Laboratory/OCDB/index.html`

Table 2. Grid values for the dust parameters around VY CMa.

τ_{rep}	T_{int}[K]	$a_{min}[\mu m]$	$a_{max}[\mu m]$	q
1.0	900	0.001	1	2.5
1.5	1000	0.01	4	3.0
2.0	1100	0.1	10	3.5
2.5	1200	1	40	4.0
3.0	1300		100	4.5
3.5	1400		400	
4.0	1500			

4. Monte Carlo Markov Chain simulations

To find the posterior distribution, P(H|E), that best matches the grid parameters with the observed data, we used the EMCCE code (**?**), a Python language implementation of the Bayesian inference and Monte Carlo Markov Chain method (MCMC). It calculates the P(H|E) of each parameter using the Bayes theorem,

$$P(H|E) = \frac{P(E|H) \times P(H)}{P(E)}\,, \tag{4}$$

where $P(H)$ is the prior that encompasses any previous information available, $P(E|H)$ is the likelihood (which is related to an adopted merit function), and $P(E)$ is a normalization factor. $P(H|E)$ is known as the posterior probability (or posterior, for short), which encompasses the information updated by an event, in our case, each event is the comparison between a combination of parameters and the observed SED. In EMCEE, the posterior is calculated from a distribution of walkers and steps, each walker being a mathematical sample whose initial position is randomly chosen and each subsequent step is decided based on a merit function (in our case, the inverse of the χ^2 [3] is used, implying that the larger the difference between the data and the model, the less likely it is for the model to represent the data). After all walkers have completed their own paths, the resulting posterior probabilities of each model parameter can either be plotted in the so-called corner plots (an example is given in Fig. **??**) or can be used to estimate the parameter value within a given range, reflecting a choice for the confidence level of the estimate. In all subsequent values and plots, we chose a confidence interval of 68 %.

5. Results

In our first tests with EMCEE and the computed grid (Table 2), we learned that when the SED data is too heterogeneous in wavelength coverage (meaning that there are high resolution regions – with many data points – and low resolution regions), EMCEE does not do a good job in fitting the entire SED as the high resolution regions dominate the χ^2 value. For this reason, we decided to bin the observed SED (Fig. 1) so that the data points become equally distributed in logarithmic scale. In this way, the weight of each SED section on the χ^2 is the same. To obtain the uncertainty of the binned data, we used the following method. The routine selects the first 20 data points, starting in the short wavelength side, subtracts the power-law $f(\lambda) = a\lambda^b$ that best describes the 20 observables and calculates the standard deviation of the data, which was adopted as the uncertainty for all the 20 data points. Then, the routine proceeds to do the same with the following 20 observables.

We computed a long MCMC simulation, considering the grid present in Table 2 and the binned SED for VY CMa, composed of 400 walkers and 5000 steps. The first 2500 steps were considered as "burn-in phase" and were removed from the chain for calculating the final probability density functions (PDFs) of each parameter. The results of the MCMC simulation are shown in Figs. 2 and **??**. They clearly indicate that the simulation converged to a best solution (Table 3).

The results suggests the present of very big grains, as discussed in Section **??**. The effect of each parameter and their correlation are further explored in Section 5.1. The best value of $q = 3.63^{+0.03}_{-0.04}$ is especially very interesting. As explained in Section 3, **?** found $q \approx 3.5$ for the interstellar medium, and the fact that our results for VY CMa matches this result is remarkable, as it may provide evidence for a commom formation on the dust grains. A study comparing the value of q for several other supergiant stars could shed a light in the contribution of RSGs to the interstellar medium or even in mass loss and dust formation.

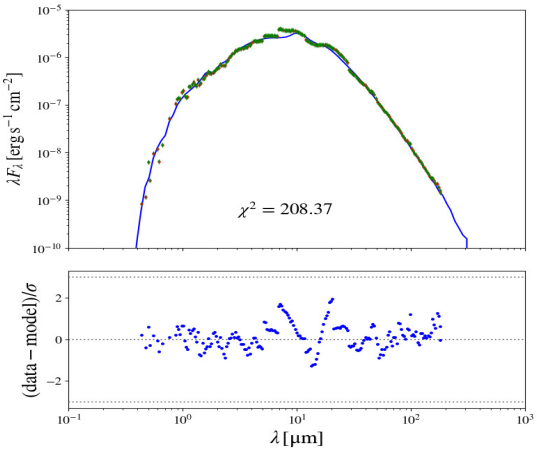

Figure 2. Model results for VY CMa. Top: comparison of the binned SED (green points) with the most-probable model (blue curve) computed with the values of Table 3. The χ^2 of this model is also indicated. Bottom: model residuals normalized by the observation uncertainties. The horizontal line indicate a 3-σ deviation from the model.

Table 3. Best values for the dust parameters around VY CMa.

$a_{min}[\mu m]$	q	τ_{rep}	$E(B-V)$	T_{int}[K]
0.47 ± 0.17	$3.63^{+0.03}_{-0.04}$	$2.42^{+0.04}_{-0.07}$	$0.58^{+0.07}_{-0.06}$	1095 ± 25
$a_{max}[\mu m]$		τ_V		$R_{int}[R_\star]$
363^{+26}_{-75}		≈ 5		≈ 13

5.1. Effect of each free parameter

To better understand the effect of each parameter on the SED, and to perform an independent verification of the results shown in Figs. 2 and **??**, we explore, in this section, how varying each parameter, while keeping the others fixed at their values of Table 3, changes the model results.

The parameter τ_{rep}, which is related to the amount of dust present, is the one that most affects the SED. Fig. **??** reveals that higher τ_{rep} means more absorption in the UV region and more emission in the IR region. This is very straightforward to understand because of the definition of τ_{rep} (Eq. 1): growing values of τ_{rep} increase the fraction of star light that is reprocessed into the IR domain, thus causing a corresponding decrease of the flux

[3] Following **?**, we adopted a variation of χ^2 that considers a distribution in a logarithmic scale, as the SED covers a dynamic range of many orders of magnitude. $\chi^2 = (\log(F_{obs}) - \log(F_{mod}))/\sigma$, where F_{obs} is the observed flux, F_{mod} is the flux of each model and σ is the uncertainties in F_{obs}.

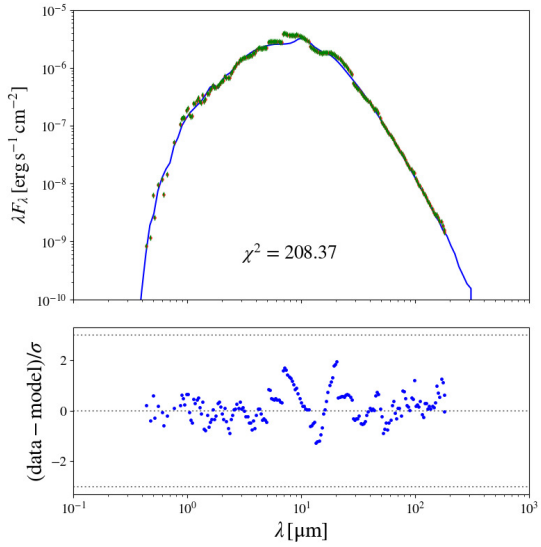

Figure 3. Corner plot representation of the output parameters of the MCMC run. The main diagonal plots show the PDFs of each parameters, with a parameter range estimate with 68% confidence level printed on top. The off-diagonal plots indicate the two-by-two correlations of each parameter.

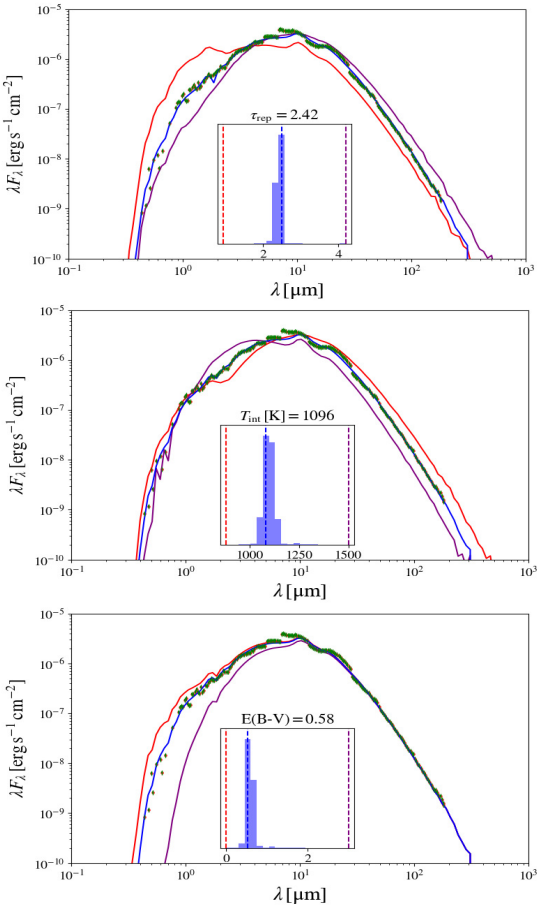

Figure 4. Effects of each free parameter (τ_{rep}, T_{int} and $E(B-V)$) on the model SED. The model in blue is the same model shown in Fig. 2. The models in red and purple represent the extreme values of each parameter in our grid.

values at shorter wavelengths. It is important to note that boundary values of τ_{rep} adopted in our grid clearly do not represent well the observations, indicating that the grid values were chosen properly.

The internal temperature of the dust (T_{int}), which is related to the internal radius of the envelope, affects mainly the peak wavelength of the dust emission, as per the well-known Wien's displacement law. In Fig. **??**, the shifting of the peak emission to longer wavelengths as the temperature decreases is visible. It is important to note that the dust temperature (around 1100 K) is much smaller than the stellar temperature (around 3500 K). Fig. **??** shows that T_{int} strongly correlates with $E(B-V)$, which is expected since larger values of T_{int} would increase the shorter wavelength flux, requiring larger values of $E(B-V)$ to compensate from it. The same occurs with T_{int} and τ_{rep}, the reason being that a higher τ_{rep} means more reprocessing, leading to excess of emission in longer wavelengths. Thus an increase in T_{int} is needed to compensate for the excess of flux.

The interstellar extinction, $E(B-V)$, is a well-known parameter whose effect is most important for shorter wavelengths. Indeed, Fig. **??** shows exactly this behavior, with the model with low $E(B-V)$ (red curve) displaying much larger flux values at the UV, visible and near IR than the model with high $E(B-V)$. As the other parameters studied so far, the range adopted for $E(B-V)$ seems to have been properly chosen.

5.1.1. Grain size

The dust grain size, a, has a more complex impact on the SED (see **?** for more details). Briefly, small grains affects more the short wavelengths, while larger grains affect more the large wavelengths. Therefore the size of the smallest grains, a_{min}, is responsible for increasing flux attenuation at short wavelengths as decreasing values are considered. However, we see, in Fig. **??**, that models with different a_{min} are very similar, indicating that this parameter may be poorly constrained by the observations.

VY CMa presents a very large flux excess in the far infrared ($\lambda > 30$ μm) as can be seen in Fig. **??** when low values of a_{max} are considered (red curve). In previous works, as **?**, the authors considered extreme large outer boundaries for the dust shell ($R_{ext} = 20000\ R_\star$) and a stepper slope in the density (Eq. 3). In this exploratory work, we tried the possibility of maintaining a small dust shell ($R_{ext} = 200\ R_\star$) and increasing the value of the largest grain in the distribution, a_{max}, in order to understand the possible outcomes. The a_{max} has a strong impact in the very long wavelengths, which is due to the fact that large grain sizes have a larger opacity at large wavelength, with a correspondingly larger emission, as per the well-known Kirchhoff's law. This analysis suggests that models with very large dust grains, 360 μm, are also able to explain the behavior of the SED of VY CMa.

Another important parameter for fitting the flux excess in the far infrared is the power-law exponent (q). As seen in Fig. **??**, if we consider a higher q (purple curve in Fig. **??**) we are not able to reproduce the excess even though considering the presence of large grains. The reason for this behaviours is that q controls the fraction of bigger grains, and thus, even when they are present, a high q will mean that due to low quantity of large grains, their presence would be negligible. Ultimately, the q parameter will control the slope of the SED in the far infrared when large grains are present. Fig. **??** shows, in fact, that a_{max} and q are strongly correlated. This happens because, as seen in Fig. **??**, increasing q means that larger a_{max} are necessary to explain the behaviour at the far infrared.

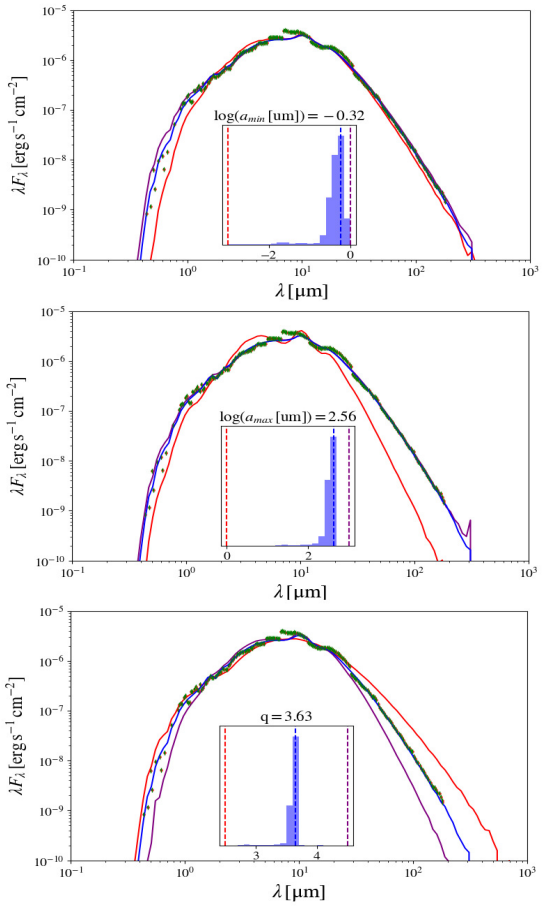

Figure 5. Same as Fig **??**, but for the parameters of the grain size distribution ($a_{\rm max}$, $a_{\rm min}$ and q).

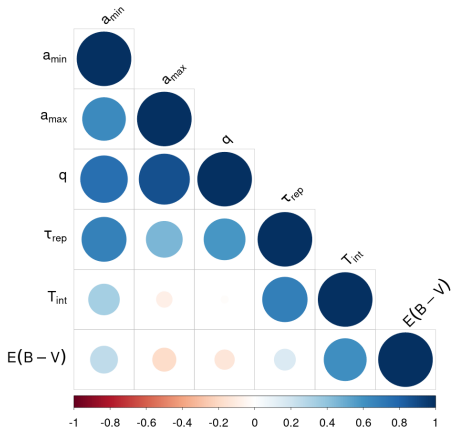

Figure 6. Correlation plot for EMCEE output. Each circle shows the value of the two-by-two correlation, computed by applying the Pearson correlation method to the final chains of the MCMC run. The larger the circle, the stronger the correlation. Positive (negative) correlations are shown in different hues of blue (red).

6. Conclusions and future steps

This work has successfully characterized the dust around VY CMa, using a new approach with the MCMC and Bayesian inference background. A remarkable fit of the entire SED was achieved with the parameters shown in Table 3. In particular, the model was able to reproduce correctly the slope and level of the SED in the far infrared. This was only achieved after adopting a grain sized distribution with the presence of very large grains ($a_{\rm max}$ = 360 μm).

The value of q shows a very interesting similarity to the value obtained by **?** in their study of the interstellar medium composition. This may indicate a connection between the grains around RSGs, such as VY CMa, and the grains in the interstellar medium, contributing to the hypothesis that they may share similar formation processes. The obtained value for $E(B-V)$ is somewhat larger than the literature value. **?** estimated the interstellar reddening ($A_{\rm V}$) to an upper limit of 1.5 (which corresponds to $E(B-V) = 0.48$, for $R_{\rm V} = 3.1$). However their models adopted much smaller grains which may explain the smaller $E(B-V)$.

One of the next steps planned for the future article is a study of the effect of $R_{\rm ext}$ as a free parameter, since a larger dust shell will have more colder grains which emits more in the far infrared, thus possibly reducing the need of (perhaps unrealistically) large grains in the model. Also, we plan to extend this study to other similar objects to explore the properties of the dust grains for a larger sample of RSGs.

Acknowledgements. T.H.A. acknowledges the public research funding in Brazil which was crucial to the development of this project, in especial FAPESP (grant 2021/01891-2 and 2018/26380-8). A.C.C. acknowledges support from CNPq (grant 311446/2019-1) and FAPESP (grants 2018/04055-8 and 2019/13354-1). This works makes use of the public available observations from the Infrared Space Observatory (ISO), from the Cassini Atlas of Stellar Spectra (CAOSS) and the photometric data present in the CDS portal. The photosphere models of Kurucz were also essential to the modelling effort of this project. The grid of models were computed using the structure of the Laboratory of Astroinformatic (LAi) from the University of São Paulo, that made this work possible.

References

Carciofi, A., Bjorkman, J., Magalhaes, A., 2004, ApJ, 604, 238.
Carciofi, A., Bjorkman, J., 2006, ApJ, 639, 1081.
Carciofi, A., Bjorkman, J., 2008, ApJ, 684, 1374.
Danchi, W., Bester, M., Degiacomi, C., Greenhill, L., Townes, C., 1994, ApJ, 107, 1469.
Draine, B., Lee, H., 1984, ApJ, 285, 89.
Foreman-Mackey, D., Hogg, D., Lang, D., Goodman, J., 2013, Astronomical Society of the Pacific, 125, 306.
Joint Iras Science Working Group 1994, VizieR Online Data Catalog:, II/125.
Kurucz, R., 1994, Smithsonian Astrophysical Observatory, 19.
Levesque, E., 2017, IOP publishing, 2514-3433, 13-14.
Mathis, J., Rumpl, W., Nordsieck, K., 1977, ApJ, 217, 425–433.
Mota, B., 2019, PhD Thesis.
Ossenkopf, V., Henning, T., Mathis, J., 1992, A&A, 261, 567.
Savage, B., Mathis, J., 1979, ARAA, 17, 73-111.
Scicluna, P., Siebenmorgen, R., Wesson, R., Blommaert, J., Kaper, M., Voshchinnikov, N., Wolf, S., A&A, 2015, 584, L10.
Shenoy, D., Humphreys, R., Jones, T., Marengo, M., Gehrz, R., Helton, L., Hoffmann, W., Skemer, A., Hinz, P., 2016, ApJ, 151, 51.
Stewart, P., Tuthill, P., Nicholson, P., Sloan, G., Hedman, M., 2015, ApJ, 221, 30.
Stothers, R., Chin, C., 1996, ApJ, 468, 842.
Wilms, J., Allen, A., McCray, R., 2000, ApJ, 542, 914-924.
Wittkowski, M., Hauschildt, P.,Arroyo-Torres, B., Marcaide, J., 2012, A&A, 540, 4.